

Computation of Energy Release Rates for Kinking Cracks based on Virtual Crack Closure Technique

De Xie¹, Anthony M. Waas^{1,2}, Khaled W. Shahwan³, Jessica A. Schroeder⁴, Raymond G. Boeman⁵

Abstract: A numerical method based on the virtual crack closure technique (VCCT) [Rybicki and Kanninen (1977)] and in conjunction with the finite element (FE) method is presented to compute strain energy release rates for cracks that kink. The method partitions the strain energy release rate and provides an efficient means to compute values of the mode I (G_I) and mode II (G_{II}) energy release rate at the tip of a kinking crack. The solution procedure is shown to be computationally efficient and operationally simple, involving only the nodal forces and displacements near the crack tip. Example problems with kinking cracks in a homogeneous material, and a layered two constituent material are presented to illustrate the current approach.

keyword: kinking crack, virtual crack closure technique, energy release rate

1 Introduction

Interest in using fracture mechanics based approaches to assess the durability and damage tolerance capability of structures is growing [Atluri (1997)]. Practical engineering structures usually possess complicated geometric configurations, nonlinear material behavior and uncertain details of the loading environment. These complications are now routinely addressed by resorting to a robust computational approach, such as the finite element (FE) method, the boundary element method and, more recently, through advances in the mesh free Galerkin method [Atluri (2004), Atluri and Shen (2002),

Belytschko, Lu, and Gu (1994), Atluri and Zhu (2000)] for stress analyses. In those instances, where failure by fracture is of concern, the virtual crack closure technique (VCCT) [Rybicki and Kanninen (1977)] and cohesive zone models are finding increased application through implementation via the FE method.

The VCCT has been widely applied to interfacial cracks to compute total and component energy release rates (G, G_I and G_{II}), based on the results from a FE stress analysis. It is a technique that is relatively insensitive to the mesh pattern and mesh density. VCCT was introduced by [Rybicki and Kanninen (1977)] for line cracks and was extended by [Shivakumar, Tan, and Newman (1988)] for planar cracks. An overview of the VCCT for interfacial cracks with a fixed (self-similar) crack front is provided by [Krueger (2002)], where a discussion with respect to different applications and a summary of historical development are presented. Recently, [Xie and Biggers (2004)] proposed a two-vector algorithm to trace a crack front so that the VCCT can be applied to moving delamination problems without using adaptive remeshing.

Slant cracks under mixed mode loading have been studied extensively. [Ishikawa (1980)] proposed a two step VCCT approach to separate the strain energy release rate components through the variation of the stiffness matrix of the crack tip elements. Combining weight function concept and VCCT, [Sha and Yang (1985)] developed procedures to calculate stress intensity factors directly and accurately. [Raju (1987)] developed the explicit expressions for strain energy release rate components for higher order and singular elements in terms of nodal forces and displacements. [Shivakumar and Raju (1992)] presented a general formulation of the equivalent domain integral method for mixed-mode fracture problems in cracked solids. For dynamic fracture mechanics, [Nishioka and Atluri (1983)] introduced a new path-independent integral which has the meaning of energy

¹Department of Aerospace Engineering, The University of Michigan Ann Arbor, MI 48109-2140, USA

²e-mail: dcw@umich.edu Fax: (734) 763-0578

³Scientific Labs, DaimlerChrysler Corporation Auburn Hills, MI 48326-2757, USA

⁴Research and Development Center, General Motors Corporation Warren, MI 48090-9055, USA

⁵Metals and Ceramics Division, Oak Ridge National Laboratory Oak Ridge, TN 37831-6053, USA

release rate for a propagating crack under mixed mode loading. In Ref [Nishioka and Atluri (1984)], Nishioka and Atluri analyzed the dynamic propagation of a slant crack under mixed-mode loading which is and has been used as a benchmark example in dynamic fracture mechanics.

The formulations developed for VCCT of a slant crack cannot be applied to a kinking crack since the former relies on self similar crack growth while in the later, the crack path changes *direction*. However, by adopting a different formulation in conjunction with the VCCT, energy release rates can be computed to evaluate the trajectory of kinking cracks and kinking crack fronts.

For simple configurations of adhesively bonded strips, with similar adherends, beam theory can be adopted [Chen and Dillard (2001)] to obtain energy release rates analytically. For planar structures, such as plates, [Hayashi and Nemat-Nasser (1981), Azhdari and Nemat-Nasser (1996)] and [He and Hutchinson (1991)] developed procedures to analytically obtain strain energy release rates by solving a series of integral equations. Based on Betti's reciprocal theorem, [Palaniswamy and Knauss (1978)] proposed an analytical expression for the total energy release rate, G , which requires a two-step analyses. [Becker, Cannon, and Ritchie (2001)], implemented a two-step VCCT to calculate the strain energy release rate for crack kinking in functionally graded materials.

In this paper, the expression for G given by [Palaniswamy and Knauss (1978)], is partitioned into mode I and mode II components and its equivalent approximation is used to develop a new one-step-VCCT for kinking cracks. The approach is validated by examining a centrally cracked plate subjected to mode I remote loading, for two different material combinations. The approach has been implemented into the commercial FE analysis software ABAQUS. The one-step VCCT for kinking cracks is found to be efficient, robust and simple to use in engineering analysis.

2 Formulation

Figure 1 shows the coordinate system for the parent interfacial crack and its child kinking crack. The parent crack lies at the interface between material (1) and (2) and has an initial length “ a ”. The crack grows into (kinks) material (1) at an angle of ω to produce a child crack with a

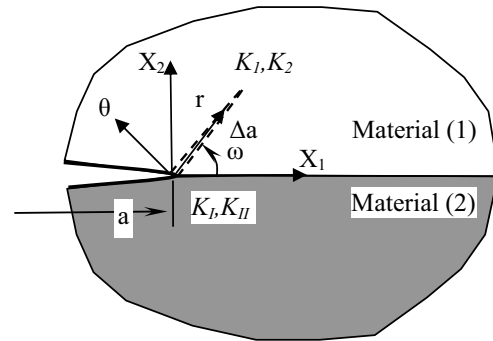


Figure 1 : Coordinate systems for interface crack and kinking crack

length “ Δa ”. The stress intensity factors K_I and K_{II} are associated with the parent crack while K_I and K_{II} correspond to the child crack. Two different implementations of the VCCT are developed; a two-step-analysis and a one-step-analysis.

2.1 Review of two-step-analysis

The energy required to create the kinking crack can be evaluated by computing the strain energy change with respect to two cases corresponding to crack length “ a ” and “ $a+\Delta a$ ”. Then the total strain energy release rate for a kinking crack can be calculated using Irwin's definition [Irwin (1956)]

$$G = \frac{U(a + \Delta a) - U(a)}{2B\Delta a} \quad (1)$$

where, B is the thickness of the cracked body. To apply a two-step-analysis, two different FEA corresponding to two different crack lengths that are infinitesimally different from each other are performed, see Figure 2 for details. The first analysis corresponds to the parent crack with crack tip configuration shown in Figure 2(a) which produces the strain energy $U(a)$. In the second analysis, a node is split to generate the kinking crack at the desired angle ω and the strain energy in this case is denoted as $U(a+\Delta a)$. Then the strain energy release rate is calculated from equation (1). Radial type meshes are highly recommended to accommodate the kinking angle, though this is not mandatory.

The strain energy release rate can also be computed locally at the crack tip. Based on Betti's reciprocal theorem, Palaniswamy and Knauss 'proposed an expression

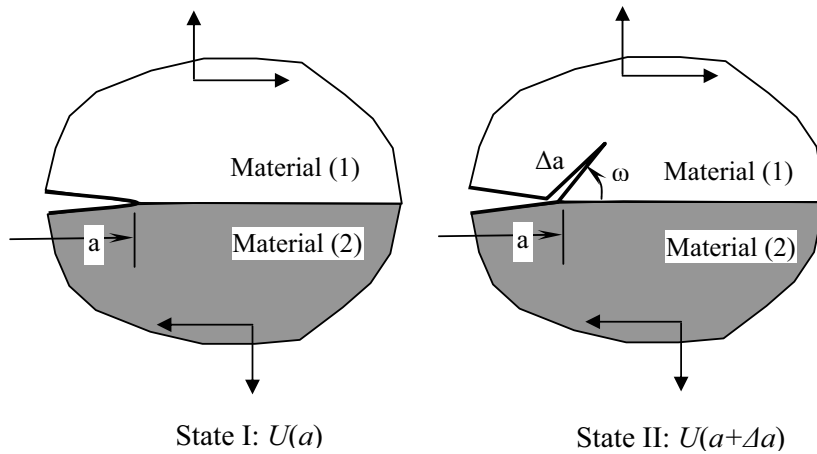


Figure 2 : Crack tip configurations for the two example problems considered

for the energy release rate of a kinking crack as

$$G(\omega) = \lim_{\Delta a \rightarrow 0} \frac{1}{2\Delta a B} \int_0^{\Delta a} \left[\sigma_{\theta\theta}^{(1)}(r, \omega) \Delta u_{\theta}^{(2)}(r, \omega) + \tau_{r\theta}^{(1)}(r, \omega) \Delta u_r^{(2)}(r, \omega) \right] dr \quad (2)$$

where $\sigma_{\theta\theta}^{(1)}(r, \omega)$ and $\tau_{r\theta}^{(1)}(r, \omega)$ are the stress components along the kinking crack line of the unkinked state (state I in Figure 2) and $\Delta u_{\theta}^{(2)}(r, \omega), \Delta u_r^{(2)}(r, \omega)$ are the opening displacement across the kinking faces corresponding to the kinked state (state II in Figure 2). In Ref [Becker, Cannon, and Ritchie (2001)], the authors used the stress field from the unkinked FEA analysis and the opening displacements from the kinked FEA analysis to perform integration on equation (2).

2.2 Partition and Approximation of $G(\omega)$

The direct integral, equation (2), involves the singular field at the crack tip. Therefore, the stress at those nodes, which are close to the crack tip, cannot be directly used in numerical integration. To overcome this, fine meshes and singular finite elements at the crack tip (see [Anderson (1991)]) are necessary. An alternative approach is to work directly with nodal forces to avoid the integration and the use of crack tip stresses. Following what has been done for straight cracks by [Rybicki and Kanninen (1977)], the following numerical evaluation of equation

(2) is proposed. Let

$$G(\omega) = G_I(\omega) + G_{II}(\omega) \quad (3a)$$

$$G_I(\omega) = \frac{F_{\theta 12}^{(1)} \Delta u_{\theta 12}^{(2)} + F_{\theta 34}^{(1)} \Delta u_{\theta 34}^{(2)}}{2\Delta a B} \quad (3b)$$

$$G_{II}(\omega) = \frac{F_{r 12}^{(1)} \Delta u_{r 12}^{(2)} + F_{r 34}^{(1)} \Delta u_{r 34}^{(2)}}{2\Delta a B} \quad (3c)$$

where, $G_I(\omega)$ and $G_{II}(\omega)$ are the mode I and mode II energy release rates for the kinking crack, respectively. Figure 3 shows the scheme for this two-step analysis. F_{θ} and F_r are the nodal forces that the FEA can provide more accurately than the local stress at the crack tip. Equation (3b) and equation (3c) provide the individual mode I and mode II crack tip energy release rates G_I and G_{II} which are desired in mixed mode fracture problems. Based on equation (3), an efficient one step analysis for energy release rate calculation for kinking cracks is proposed next.

2.3 One-step-analysis approach

The basic idea for the one step analysis (Figure 4) is to replace the displacement opening along the kinking crack line in the second step ($\Delta u_r^{(2)}, \Delta u_{\theta}^{(2)}$) in equation (3) with the displacement opening behind the parent crack in the first step ($\Delta u^{(1)}, \Delta v^{(1)}$). Then all the variables in equation (3) are computed within one step. The displacement fields at a crack tip can be expressed as [Anderson

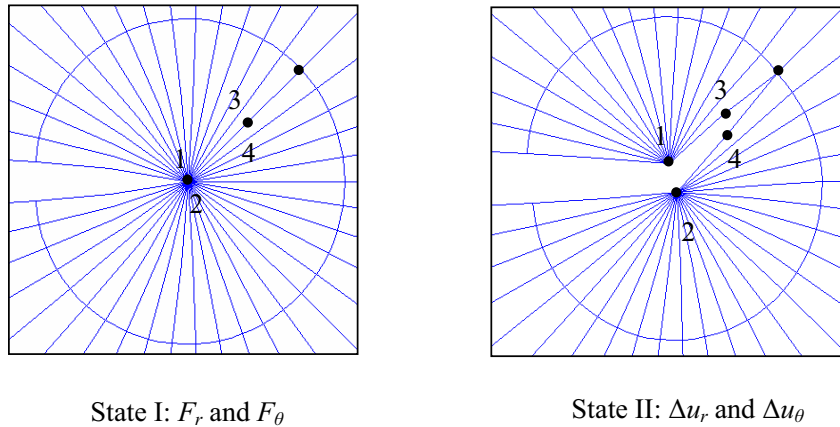


Figure 3 : Crack tip configurations for local analysis of kinking cracks

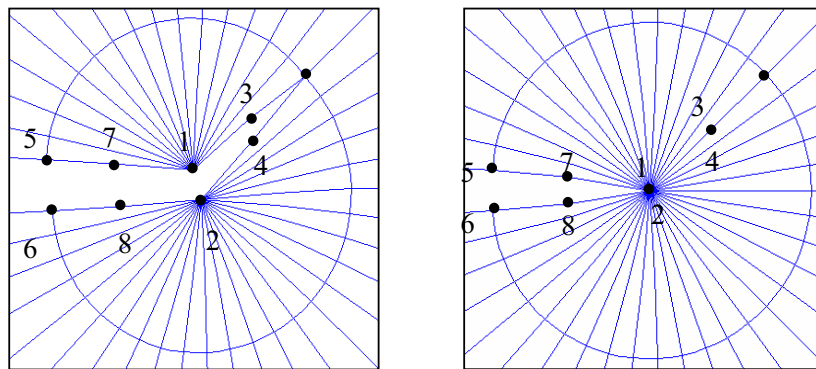


Figure 4 : One step analysis which relates node pairs (1,2) to (5,6) and (3,4) to (7,8)

(1991)],

$$u = \frac{K_I}{2\mu} \sqrt{\frac{r}{2\pi}} \cos\left(\frac{\theta}{2}\right) \left[\kappa - 1 + 2\sin^2\left(\frac{\theta}{2}\right) \right] + \frac{K_{II}}{2\mu} \sqrt{\frac{r}{2\pi}} \sin\left(\frac{\theta}{2}\right) \left[\kappa + 1 + 2\cos^2\left(\frac{\theta}{2}\right) \right] \quad (4a)$$

$$v = \frac{K_I}{2\mu} \sqrt{\frac{r}{2\pi}} \sin\left(\frac{\theta}{2}\right) \left[\kappa + 1 - 2\cos^2\left(\frac{\theta}{2}\right) \right] - \frac{K_{II}}{2\mu} \sqrt{\frac{r}{2\pi}} \cos\left(\frac{\theta}{2}\right) \left[\kappa - 1 - 2\sin^2\left(\frac{\theta}{2}\right) \right] \quad (4b)$$

where, μ is the shear modulus, $\kappa = (3-\nu)/(1+\nu)$ for plane stress, and ν is the Poisson's ratio. For the parent interfacial crack, the displacement components of the upper ($\theta = \pi, \kappa = \kappa_1, \mu = \mu_1$) and lower ($\theta = -\pi, \kappa = \kappa_2, \mu = \mu_2$) crack surfaces are

$$u^+ = \frac{\kappa_1 + 1}{2\mu_1} \sqrt{\frac{|X_1|}{2\pi}} K_{II} \quad ; \quad v^+ = \frac{\kappa_1 + 1}{2\mu_1} \sqrt{\frac{|X_1|}{2\pi}} K_I \quad (5a)$$

$$u^- = -\frac{\kappa_2 + 1}{2\mu_2} \sqrt{\frac{|X_1|}{2\pi}} K_{II}; \quad v^- = -\frac{\kappa_2 + 1}{2\mu_2} \sqrt{\frac{|X_1|}{2\pi}} K_I \quad (5b)$$

The crack opening, for the parent crack, in state (1) is

$$\Delta u^{(1)} = u^+ - u^- = \left(\frac{\kappa_1 + 1}{2\mu_1} + \frac{\kappa_2 + 1}{2\mu_2} \right) \sqrt{\frac{|X_1|}{2\pi}} K_{II} \quad (6a)$$

$$\Delta v^{(1)} = v^+ - v^- = \left(\frac{\kappa_1 + 1}{2\mu_1} + \frac{\kappa_2 + 1}{2\mu_2} \right) \sqrt{\frac{|X_1|}{2\pi}} K_I \quad (6b)$$

For the child-kinking crack, the displacement components of the upper and lower crack surfaces are taken as

$$u_r^+ = \frac{\kappa_1 + 1}{2\mu_1} \sqrt{\frac{r}{2\pi}} K_2(\omega); \quad u_\theta^+ = \frac{\kappa_1 + 1}{2\mu_1} \sqrt{\frac{r}{2\pi}} K_1(\omega) \quad (7a)$$

$$u_r^- = -\frac{\frac{\kappa_1+1}{2\mu_1}\omega + \frac{\kappa_2+1}{2\mu_2}\pi}{\omega + \pi} \sqrt{\frac{r}{2\pi}} K_2(\omega); \quad (11)$$

$$u_\theta^- = -\frac{\frac{\kappa_1+1}{2\mu_1}\omega + \frac{\kappa_2+1}{2\mu_2}\pi}{\omega + \pi} \sqrt{\frac{r}{2\pi}} K_1(\omega) \quad (7b)$$

and the crack opening for the kinking crack at state (2) is

$$\Delta u_r^{(2)} = u_r^+ - u_r^- = \frac{\frac{\kappa_1+1}{2\mu_1}(2\omega + \pi) + \frac{\kappa_2+1}{2\mu_2}\pi}{\omega + \pi} \sqrt{\frac{r}{2\pi}} K_2(\omega) \quad (8a)$$

$$\Delta u_\theta^{(2)} = u_\theta^+ - u_\theta^- = \frac{\frac{\kappa_1+1}{2\mu_1}(2\omega + \pi) + \frac{\kappa_2+1}{2\mu_2}\pi}{\omega + \pi} \sqrt{\frac{r}{2\pi}} K_1(\omega) \quad (8b)$$

At the parent crack tip, the stress components having contributions to the kinking child crack, in a polar coordinate system, with origin at the crack tip, for mixed mode loading are given by [Anderson (1991)]

$$\sigma_{\omega\omega} = \frac{K_I}{\sqrt{2\pi r}} C_{11}(\omega) + \frac{K_{II}}{\sqrt{2\pi r}} C_{12}(\omega) \quad (9a)$$

$$\tau_{r\omega} = \frac{K_I}{\sqrt{2\pi r}} C_{21}(\omega) + \frac{K_{II}}{\sqrt{2\pi r}} C_{22}(\omega) \quad (9b)$$

where

$$C_{11}(\omega) = \frac{1}{4} \left[3 \cos\left(\frac{\omega}{2}\right) + \cos\left(\frac{3\omega}{2}\right) \right]; \quad (10a)$$

$$C_{12}(\omega) = -\frac{1}{4} \left[3 \sin\left(\frac{\omega}{2}\right) + 3 \sin\left(\frac{3\omega}{2}\right) \right] \quad (10b)$$

$$C_{21}(\omega) = \frac{1}{4} \left[\sin\left(\frac{\omega}{2}\right) + \sin\left(\frac{3\omega}{2}\right) \right]; \quad (10c)$$

$$C_{22}(\omega) = \frac{1}{4} \left[\cos\left(\frac{\omega}{2}\right) + 3 \cos\left(\frac{3\omega}{2}\right) \right] \quad (10d)$$

Suppose that an infinitesimal kinked crack initiates at an angle ω from the parent crack, as shown in Figure 1. The local stress intensity factors at the tip of this kinked crack differ from those of the parent crack. Define the following two stress intensity factors, $K_1(\omega)$ and $K_2(\omega)$, associated with the kinked crack at an arbitrary angle ω ,

$$K_1(\omega) = \lim_{r \rightarrow 0} \left(\sqrt{2\pi r} \sigma_{\omega\omega} \right) \quad K_2(\omega) = \lim_{r \rightarrow 0} \left(\sqrt{2\pi r} \tau_{r\omega} \right)$$

where r is the distance from the parent crack tip. Using this definition, one can show that

$$K_1(\omega) = C_{11}K_I + C_{12}K_{II} \quad (12a)$$

$$K_2(\omega) = C_{21}K_I + C_{22}K_{II} \quad (12b)$$

Then, by substituting (12) and (6) into (8), we have

$$\Delta u_r^{(2)} = \frac{2\omega + \pi + \gamma\pi}{(\omega + \pi)(1 + \gamma)} \sqrt{\frac{r}{|X_1|}} \left(C_{21}\Delta v^{(1)} + C_{22}\Delta u^{(1)} \right) \quad (13a)$$

$$\Delta u_\theta^{(2)} = \frac{2\omega + \pi + \gamma\pi}{(\omega + \pi)(1 + \gamma)} \sqrt{\frac{r}{|X_1|}} \left(C_{11}\Delta v^{(1)} + C_{12}\Delta u^{(1)} \right) \quad (13b)$$

where

$$\gamma = \frac{\kappa_2 + 1}{2\mu_2} / \frac{\kappa_1 + 1}{2\mu_1}$$

Now, the displacement components at step two ($\Delta u_r^{(2)}, \Delta u_\theta^{(2)}$) can be replaced by those at step one ($\Delta u^{(1)}, \Delta v^{(1)}$) by using Equation (13). Therefore, the virtual crack closure technique can be applied within a one step analysis.

2.4 Radial Type Mesh

Although it is not mandatory, the radial type mesh is highly recommended. By using the radial type meshes shown in Figure 4, the node pair (1,2) has the same distance to the kinking crack tip (r) as the node pair (5,6) has to the parent crack tip ($|X_1|$). Therefore, the term $\sqrt{r/|X_1|}$ can be cancelled in equation (13) and one can have

$$\Delta u_{r12}^{(2)} = A \left(C_{21}\Delta v_{56}^{(1)} + C_{22}\Delta u_{56}^{(1)} \right) \quad (14a)$$

$$\Delta u_{\theta 12}^{(2)} = A \left(C_{11}\Delta v_{56}^{(1)} + C_{12}\Delta u_{56}^{(1)} \right) \quad (14b)$$

where

$$A = \frac{2\omega + \pi + \gamma\pi}{(\omega + \pi)(1 + \gamma)}$$

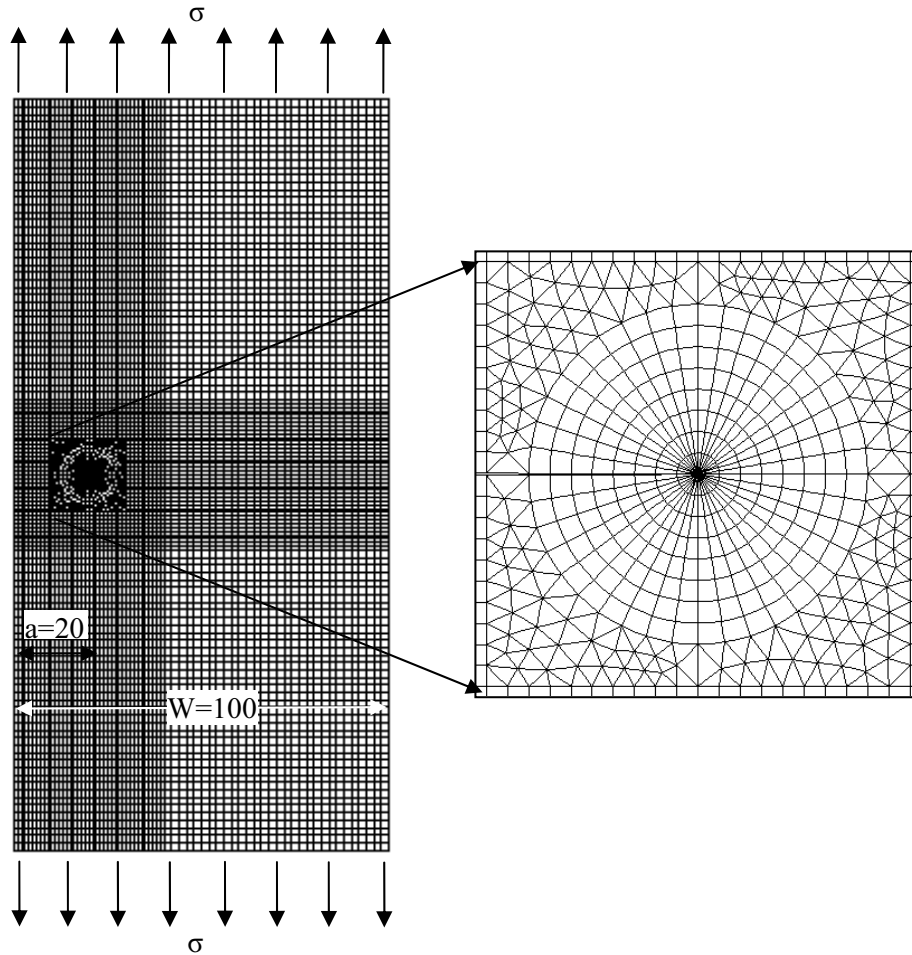


Figure 5 : FEA mesh for the verification example

A similar procedure can be applied to node pairs (3, 4) and (7, 8),

$$\Delta u_{r34}^{(2)} = A \left(C_{21} \Delta v_{78}^{(1)} + C_{22} \Delta u_{78}^{(1)} \right) \quad (15a)$$

$$\Delta u_{\theta 34}^{(2)} = A \left(C_{11} \Delta v_{78}^{(1)} + C_{12} \Delta u_{78}^{(1)} \right) \quad (15b)$$

By substituting (14) and (15) into (3), a one step VCCT provides,

$$G_I(\omega) = \frac{A}{2\Delta a B} \left[F_{\theta 12}^{(1)} \left(C_{11} \Delta v_{56}^{(1)} + C_{12} \Delta u_{56}^{(1)} \right) + F_{\theta 34}^{(1)} \left(C_{11} \Delta v_{78}^{(1)} + C_{12} \Delta u_{78}^{(1)} \right) \right] \quad (16a)$$

$$G_{II}(\omega) = \frac{A}{2\Delta a B} \left[F_{r 12}^{(1)} \left(C_{21} \Delta v_{56}^{(1)} + C_{22} \Delta u_{56}^{(1)} \right) + F_{r 34}^{(1)} \left(C_{21} \Delta v_{78}^{(1)} + C_{22} \Delta u_{78}^{(1)} \right) \right] \quad (16b)$$

The nodal forces F_r and F_θ in the local coordinate system can be expressed through F_x and F_y in the global coordinate system as

$$F_r = F_y \sin \omega + F_x \cos \omega \quad F_\theta = F_y \cos \omega - F_x \sin \omega$$

Nodal forces (F_x, F_y) and displacement openings ($\Delta u, \Delta v$) can be read directly from the FEA output. These values then are the input data to compute strain energy release rates $G_I(\omega)$ and $G_{II}(\omega)$.

The above procedure for the one step VCCT has been implemented into ABAQUS with the use of a user subroutine that allows the computation of $G_I(\omega)$ and $G_{II}(\omega)$ simultaneously with the stress analysis performed by ABAQUS.

Table 1 : Strain energy release rate for cracks at $\omega = 0^\circ$ (unit: N/mm)

	Analytical	Two-step Approach		J-integral From ABAQUS
		Eq. (1)	Eq. (3)	
Case (a)	6.498	6.612	6.612	6.507
Case (b)	3.938	3.886	3.886	3.829

3 Verification

The proposed one step and two-step VCCT for kinking cracks were validated by an example of a centrally cracked plate subjected to a normal tensile stress $\sigma_\infty=10\text{MPa}$ as shown in Figure 5. The half crack length, a , is taken to be 20mm and the plate width, W , is taken as 100mm. The finite element mesh of the panel is also shown in Figure 5. Two different cases were studied:

- Case (a): Homogeneous material $E=1000\text{ MPa}$, $\nu=0.25$
- Case (b): Bi-material $E_1=1000\text{ MPa}$, $\nu_1=0.25$; $E_2=4000\text{MPa}$, $\nu_2=0.25$

Due to geometric and material symmetry conditions, only one half of the panel needs to be considered. A total of 8660 elements with 27000 nodes are employed. The ABAQUS standard quadratic plane stress elements ‘‘CPS8’’ and ‘‘CPS6’’ are used.

First, the two-step analysis using equation (3) was used to compute the total energy release rate and compared with an analytical solution. As the kinking angle is zero, the analytical solution for the total energy release rate for a bi-material crack is

$$G = (1 - \beta^2)(1 + 4\epsilon^2) \frac{[Y\sigma\sqrt{\pi a}]^2}{E_*}$$

where β and ϵ are the bi-material [Dundurs (1969)] constants,

$$\beta = \frac{\mu_1(\kappa_2 - 1) - \mu_2(\kappa_1 - 1)}{\mu_1(\kappa_2 + 1) + \mu_2(\kappa_1 + 1)}$$

$$\epsilon = \frac{1}{2\pi} \ln \left(\frac{1 - \beta}{1 + \beta} \right)$$

$$\frac{1}{E_*} = \frac{1}{2} \left(\frac{1}{E_1} + \frac{1}{E_2} \right)$$

Y is a geometry modification factor

$$Y = \sqrt{\frac{2W}{\pi a} \tan \left(\frac{\pi a}{2W} \right)}$$

When the two materials in a bi-material are identical, $\epsilon = \beta = 0$, and G becomes

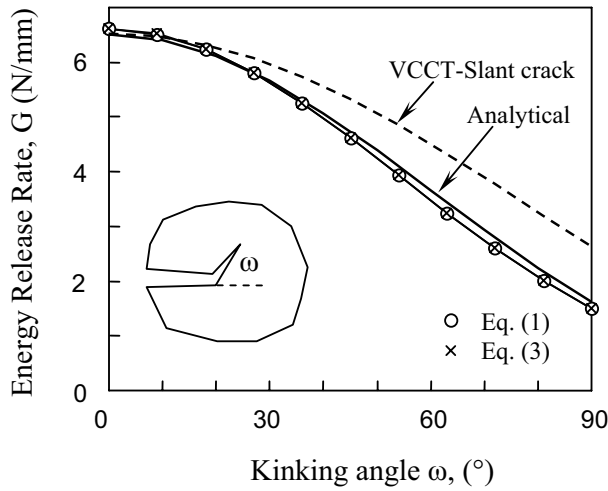
$$G = \frac{[Y\sigma\sqrt{\pi a}]^2}{E}$$

The numerical results are compared with the analytical solutions for the crack along the interface ($\omega = 0^\circ$). Computed results are given in Table 1. The analytical solution, and the two step VCCT based on equations (1) and (3) are compared, along with a J-integral [ABAQUS] computation from ABAQUS. It is seen that the present two-step VCCT predictions are in excellent agreement with the closed form solution.

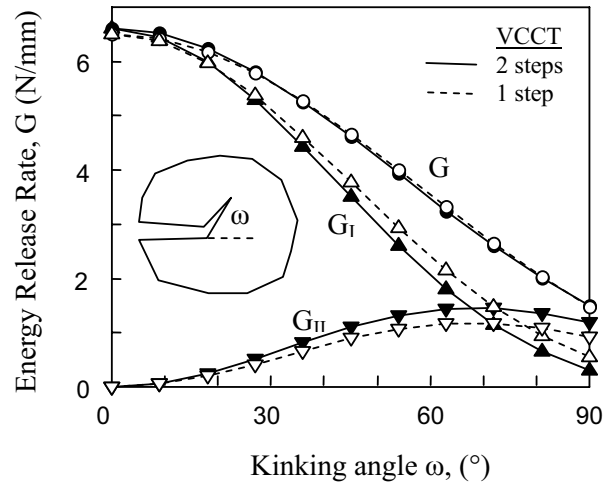
When the crack kinking angle is not zero, the analytical expression for G in a homogeneous material is

$$G = [C_{11}^2(\omega) + C_{21}^2(\omega)] \frac{[Y\sigma\sqrt{\pi a}]^2}{E},$$

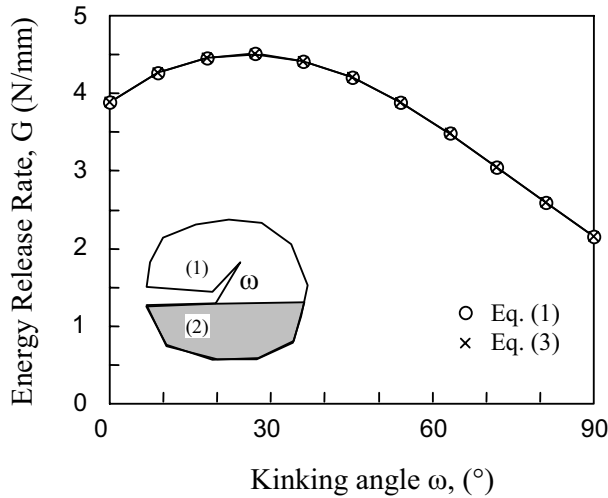
where, $C_{11}(\omega)$ and $C_{21}(\omega)$ is as shown in equation (10). The analytical solution and calculations based on equations (1) and (2) are plotted in Figure 6(a). The results obtained from VCCT for a slant crack are also included in this figure. It is clear that slant crack results based on straight crack extension are not applicable to the kinking crack problem. For the bi-material case, only calculations based on equations (1) and (2) are plotted in Figure 6(b). One can see that Equation (1) and equation (3) give identical results for both material cases as expected since they are equivalent based on Betti’s reciprocal theorem. Equation (1), equation (3) and the analytical solution all agree very well for the full range of kinking angles for the homogeneous material.



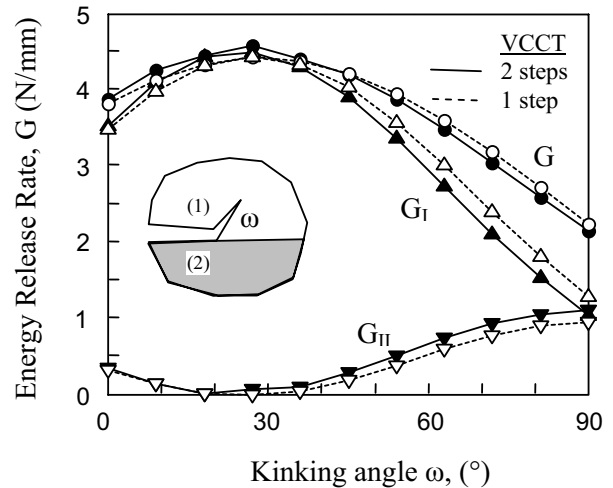
(a) Homogenous material



(a) Homogenous material



(b) Bi-material



(b) Bi-material

Figure 6 : Results for the strain energy release rate computed using equation (3)

Figure 7 : Strain energy release rates using the one step VCCT

Compared to the expression given in (1), the expression in (3) has the advantage of providing the partition of the energy release rate. Compared to the expression in (2), G given in (1) avoids the complications associated with the integration. Therefore, the two-step VCCT is an accurate, efficient and powerful tool for computing partitioned energy release rates for crack kinking problems.

Next, the one step VCCT predictions are compared against the two steps VCCT given by equation (3). The total strain energy release rates obtained from the analytical solution and the two VCCT approaches are listed in Table 2 for a zero crack-kinking angle. It is seen that the present one-step approach is as accurate as the two-step VCCT. Differences persist, but these are small compared to the efficiency gained in using a one-step VCCT com-

Table 2 : Strain energy release rate for cracks at $\omega = 0^\circ$ (unit: N/mm)

	Analytical	Two-step-analysis	One-step-analysis
Case (a)	6.498	6.612	6.515
Case (b)	3.938	3.886	3.823

putation compared against a two-step VCCT approach.

Partition of the energy release rate is also studied. For non-zero kink angles, Figure 7 shows good agreement between the two VCCT approaches for both material case (a) and material case (b). This agreement thus indicates that the one-step VCCT approach is an efficient and accurate procedure for computing the total and component energy release rates for kinking cracks.

4 Conclusions

A new computational procedure to compute the energy release rate in a two-dimensional setting for kinking cracks based on the virtual crack closure technique has been presented and validated. The present approach can provide partitioned strain energy release rates for each individual fracture mode. Other approaches to compute strain energy release rates involve complications associated with direct integration of the singular fields in and around the crack-tip. The present approach avoids these complications and can be conveniently implemented in commercial FEA software such as ABAQUS. The one-step VCCT is an accurate, efficient and powerful tool in engineering analysis for crack kinking problems.

Acknowledgement: The authors wish to thank the DOE program management team and the Board and staff of the Automotive Composites Consortium. This work was sponsored by the Automotive Composites Consortium Joining Work Group and the U. S. Department of Energy, Office of Energy Efficiency and Renewable Energy, FreedomCAR and Vehicle Technologies, Automotive Lightweighting Materials Program, under Cooperative Agreement number DE-FC05-95OR22363. DX and AMW wish to thank the Aerospace Engineering Department at the University of Michigan.

References

ABAQUS: ABAQUS Theory Manual, v6.3, Pawtucket, RI.
Anderson, T. L. (1991): Fracture Mechanics - Funda-

mentals and Applications, CRC Press.

Atluri, S. N. (2004): *The Meshless Local Petrov-Galerkin (MLPG) Method for Domain & Boundary Discretizations*, Tech Science Press, Forsyth, GA.

Atluri, S. N. (1997): Structural Integrity and Durability, Tech Science Press, Forsyth, GA.

Atluri, S. N.; Zhu, T. L. (2000): New concepts in meshless methods, *Int. J. Numerical Methods Eng.*, 47: 537-556.

Atluri, S. N.; Shen, S. (2002): The meshless local Petrov-Galerkin (MLPG) method: A simple & less-costly alternative to the finite element and boundary element methods. *CMES: Computer Modeling in Engineering & Sciences*, vol. 3, no. 1, pp. 11-52

Azhdari, A.; Nemat-Nasser, S. (1996): Energy-release rate and crack kinking in anisotropic brittle solids, *J. Mech. Phys. Solids*, 44: 929-951.

Becker, Jr. T. L.; Cannon, R. M.; Ritchie, R. O. (2001): Finite crack kinking and T-stresses in functionally graded materials, *International Journal of Solids and Structures*, 38: 5545-5563.

Belytschko, T.; Lu, Y. Y.; Gu, L. (1994): Element-Free Galerkin Methods, *International Journal for Numerical Methods in Engineering*, 37: 229-256.

Chen, B.; Dillard, D. A. (2001): Numerical analysis of directionally unstable crack propagation in adhesively bonded joints, *International Journal of Solids and Structures*, 38: 6907-6924.

Dundurs, J. (1969): Edge-bonded dissimilar orthotropic elastic wedges, *J. Appl. Mech.*, 36: 650-652.

Hayashi, K.; Nemat-Nasser, S. (1981): Energy-release rate and crack kinking, *International Journal of Solids and Structures*, 17: 107-114.

He, M. Y.; Hutchinson, J. W. (1991): Kinking of a crack out of an interface: role of in-plane stress, *J. Amer. Ceram. Soc.*, 74: 767-771.

Irwin, G. R. (1956): Onset of fast crack propagation in high strength steel and aluminum alloys, Sagamore Research Conference Proceedings, vol.2, 289-305.

Ishikawa, H. (1980): A finite element analysis of stress intensity factors for combined tensile and shear loading by only a virtual crack extension, *Int J Fracture*, 16:R243-R246.

Krueger, R. (2002): The virtual crack closure technique: History, approach and applications, ICASE Report 2002-10, NASA/CR-2002-211628.

Nishioka, T.; Atluri, S. N. (1983): Path-independent integrals, energy release rates, and general solutions of near-tip fields in mixed-mode dynamic fracture mechanics, *Engineering Fracture Mechanics*, 18:1-22.

Nishioka, T.; Atluri, S. N. (1984): On the computation of mixed-mode K-factors for a dynamically propagating crack, using path-independent integrals J_k , *Engineering Fracture Mechanics*, 20:193-208.

Palaniswamy, K.; Knauss, W. G. (1978): On the problem of crack extension in brittle solids under general loading. In: Nemat-Nassar, S. (Ed.), *Mechanics Today*, vol. 4. Pergamon Press, New York.

Raju, I. S. (1987): Calculation of strain-energy release rates with higher order and singular finite element, *Engineering Fracture Mechanics*, 28:251-274.

Rybicki, E. F.; Kanninen, M. F. (1977): A Finite element calculation of stress intensity factors by a modified crack closure integral, *Engineering Fracture Mechanics*, 9: 931-938.

Sha, G. T.; Yang, C. T. (1985): Weight function calculations for mixed-mode fracture problems with the virtual crack extension technique, *Engineering Fracture Mechanics*, 21:1119-1149.

Shivakumar, K. N.; Tan, P. W.; Newman, Jr. J. C. (1988): A virtual crack-closure technique for calculating stress intensity factors for cracked three dimensional bodies, *International Journal of Fracture*, 36: R43-R50.

Shivakumar, K. N.; Raju, I. S. (1992): An equivalent domain integral method for three-dimensional mixed-mode fracture problems, *Engineering Fracture Mechanics*, 42:935-959.

Xie, D.; Biggers, Jr. S. B. (2004): Strain energy release rate calculation for a moving delamination front of arbitrary shape based on Virtual Crack Closure Technique, *Engineering Fracture Mechanics*, in review.